Small-angle x-ray scattering study of kinetics of spinodal decomposition in *N*-isopropylacrylamide gels

Guangdong Liao,[1] Yonglin Xie,[1,2] and Karl F. Ludwig, Jr.,[1] Rama Bansil,[1] and Patrick Gallagher[1,3]
[1]*Center for Polymer Studies and Department of Physics, Boston University, Boston, Massachusetts 02215*
[2]*Xerox Corporation, Rochester, New York*
[3]*National Institute of Standards and Technology, Gaithersburg, Maryland*
(Received 30 December 1998)

We present synchrotron-based time-resolved small-angle x-ray scattering (SAXS) measurements of spinodal decomposition in a covalently cross-linked N-isopropylacrylamide gel. The range of wave numbers examined is well beyond the position of the maximum in the structure factor $S(q,t)$. The equilibrium structure factor is described by the sum of a Lorentzian and a Gaussian. Following a temperature jump into the two phase region, the scattered intensity increases with time and eventually saturates. For early times the linear Cahn-Hilliard-Cook (CHC) theory can be used to describe the time evolution of the scattered intensity. From this analysis we found that the growth rate $R(q)$ is linearly dependent on q^2, in agreement with mean-field theoretical predictions. However the Onsager transport coefficient $\Lambda(q) \sim q^{-4}$, which is stronger than the q dependence predicted by the mean-field theory. We found that the growth rate $R(q)>0$, even though the wave numbers q probed by SAXS are greater than $\sqrt{2}q_m$ where q_m is the position of the peak of $S(q,t)$, also in agreement with the mean-field predictions for a deep quench. We have also examined the range of validity of the linear CHC theory, and found that its breakdown occurs earlier at higher wave numbers. At later times, a pinning of the structure was observed. The relaxation to a final, microphase-separated morphology is faster and occurs earlier at the highest wave numbers, which probe length scales comparable to the average distance between crosslinks. [S1063-651X(99)12910-6]

PACS number(s): 82.70.Gg, 64.75.+g

I. INTRODUCTION

Numerous studies have shown that polymer gels can undergo either a discrete or a continuous volume transition (commonly referred to as the gel collapse or volume phase transition) triggered by changing temperature, *p*H, ionic content, or other parameters. The equilibrium aspects of the volume phase transition have been extensively investigated. The basic mechanism of the volume change in the gel can be described using the Flory-Huggins formulation of the polymer solution phase behavior and the theory of rubber elasticity. Using these ideas, Dusek and Patterson [1] predicted a first-order phase transition between a concentrated phase and a dilute phase. Tanaka [2] demonstrated the existence of critical fluctuations in acrylamide gels, and subsequent work led to the determination of a spinodal (the curve separating metastable and unstable regions in a mean-field phase diagram) in these transitions. Although, in these respects, the thermodynamic behavior is similar to the phase separation in polymer solutions, the existence of a network in the polymer gel precludes a macroscopic phase transition into concentrated and dilute phases; rather the system exhibits microphase separation.

The kinetics of macroscopic gel swelling/and shrinking, involving solvent absorption/and desorption, is a diffusive process directly related to the viscoelastic properties of the system and the friction between the network and the solvent, with the relaxation time depending on the dimensions and the shape of the gel [3]. This macroscopic collapse occurs on time scales from hours to days. On the other hand, there is a fast kinetics associated with the growth of concentration fluctuations in the vicinity of a spinodal. This process of spinodal decomposition, similar to that in polymer solutions, also occurs in gels if the gel is suddenly quenched from the one-phase region to the unstable region of the phase diagram along an isochoric path. However, the kinetics of spinodal decomposition in gels might differ from that in polymer solutions because of the influence of the network elasticity on the growth of fluctuations.

Hydrogels made with N-isopropyl-acrylamide (NIPA) undergo this transition upon heating [4], because NIPA is a hydrophobic polymer and exhibits a lower critical solution temperature. The phase diagram of NIPA gels has been accurately measured and agrees with calculations based on Flory-Huggins theory [5]. The equilibrium structure factors and dynamics of concentration fluctuations in NIPA gels as a function of the degree of swelling have been extensively studied [6]. A few studies of the early stages of the spinodal decomposition process in NIPA gels have been reported [5,7,8]. Small-angle light scattering (SALS) measurements show features typical of spinodal decomposition, i.e., a peak in the structure factor, which grows in intensity and shifts to smaller wave numbers as the size of the phase-separated domains increases with time. In our earlier work, using SALS [8], we showed that the early time evolution of phase separation can be described in terms of the linear Cahn-Hilliard-Cook theory.

In this paper we present small-angle x-ray scattering (SAXS) measurements on NIPA gels to examine the evolution of structure on length scales comparable to the correlation length of solution like concentration fluctuations in the gel and the average distance between crosslinks in the gel. To the best of our knowledge, these questions have not been

addressed for gels, although SAXS has been used to study the early stages of phase separation kinetics on length scales comparable to the radius of gyration of the polymer chain, R_g, in polymer blends and polymer solutions [9]. In systems with much slower kinetics, time-resolved small-angle neutron scattering (SANS) [10,11] has been used to probe the time evolution of the internal scattering (i.e., the scattering due to local composition fluctuations within each phase-separated domain) as well as the time-dependent scattering from the growing domains.

II. THEORETICAL BACKGROUND

The early stages of spinodal decomposition have often been analyzed using the linear Cahn-Hillard-Cook (CHC) [12,13] description, based on the the linearization of a generalized Langevin equation. The linear CHC model has been modified by de Gennes [14], Pincus [15], and Binder [16], using the mean-field theory of polymer blends to describe the time evolution of the structure factor in blends undergoing spinodal decomposition. This mean-field treatment can also be used for polymer solutions in a solvent [16] and may be applicable to gels, since a modified Flory-Huggins free energy works reasonably well in describing the equilibrium behavior of the gel collapse phase transition [5].

According to the CHC model a linearized equation for the time evolution of the structure factor $S(q,t)$ in a polymer system undergoing spinodal decomposition can be written

$$\frac{\partial S(q,t)}{\partial t} = 2R(q)S(q,t) + 2k_B T\Lambda(q)q^2, \tag{1}$$

where $\Lambda(q)$, the Onsager coefficient, is the Fourier transform of the nonlocal mobility, k_B is the Boltzmann constant, T is the temperature to which the system is quenched, and $R(q)$ is the growth rate.

The solution of Eq. (1) can be written

$$S(q,t) = S_\infty(q) + [S(q,0) - S_\infty(q)]e^{2R(q)t}, \tag{2}$$

where $S(q,0)$ is the initial structure factor just after a quench into the unstable two phase region, and $S_\infty(q)$ is a virtual structure factor for a quench into the spinodal region. According to the linear theory, $S_\infty(q)$ is negative, being the extrapolated final collective structure factor at the quench temperature, and never reached physically. The growth rate $R(q)$, the Onsager coefficient $\Lambda(q)$ and the virtual structure factor are related to each other by

$$R(q) = -k_B T\Lambda(q)q^2 S_\infty^{-1}(q). \tag{3}$$

In the low wave number regime ($qR_g \ll 1$) typically probed by light scattering $\Lambda(q)$ is independent of q, and this gives rise to a q-independent apparent diffusion constant D related to the growth rate $R(q)$ via $R(q) = Dq^2[1 - q^2/q_c^2]$, where q_c represents the cutoff wave number beyond which concentration fluctuations decay rather than grow. In the linear CHC theory q_c is related to the wave number of maximum growth rate $q_m = q_c/\sqrt{2}$. However, in the high-q regime probed by SAXS and SANS, several studies have shown that $\Lambda(q)$ has a considerable q dependence in the range $qR_g \geqslant 1$ [9–11]. The mean-field approach of Binder predicted $\Lambda(q) \sim q^{-2}$ for high q. In this same q range the thermal concentration fluctuations in the single phase region affect the growth of concentration fluctuations in spinodal decomposition due to the thermal noise term [the so-called Cook term in Eq. (1)]. Furthermore, for deep quenches, Binder [16] showed that $q_m \ll q_c$.

III. EXPERIMENT

A. Sample preparation

NIPA gels were polymerized at room temperature (20 °C) by the procedure used by Shibayama *et al.* [6] with 7.8 g of recrystallized N-isopropylacrylamide (Kodak Corp.), 0.345 g of methylenebisacrylamide (BIS) as cross linker, and 40 mg of persulfate as an initiator dissolved in 100 mL of distilled water. Nitrogen gas was bubbled through the solution to remove the dissolved oxygen for about 10 min. 240 μL of tetramethylethylenediamine was added into the solution as an accelerator. After the solution was completely mixed, it was placed into the x-ray scattering cell. The pre-gel solution was inject between two thin flat kapton windows glued to copper plates before the sample turned into a gel. The sample thickness of approximately 2 mm was maintained by using an O ring between the kapton windows. Within half an hour, a gel was formed at room temperature. The cloud point temperature of the sample determined by measurements of turbidity was found to be around 34.5 °C. We found that for gels with a fixed total monomer concentration, the cloud point depends slightly on the cross-link content, increasing from 32.8 °C for a sample with 0% BIS (linear polymer) to 34.5 °C for the 4% sample used in this study. In a small-angle light scattering study of a NIPA gel with the same total monomer concentration as used here but a lower crosslink content [8] we found the cloud point at 32.8 °C and a classic spinodal behavior (peak at finite q) for a quench to 33.85 °C. Samples of comparable compositions were used in the SANS study by Shibayama *et al.* [6]. The spinodal temperature of their samples, measured by dynamic light scattering, were in the range of 33–35 °C. It is important to note that Shibayama *et al.* [6] swelled the samples in D_2O, whereas we used our gels in the as-prepared state in H_2O without swelling to equilibrium. Thus for a deep quench, say around 40 °C, the initial process of phase separation in these gels will occur by the mechanism of spinodal decomposition.

B. SAXS experiment

The SAXS experiments reported here were performed at the X-20C beamline of the National Synchrotron Light Source at Brookhaven National Laboratory. This beamline is ideally suited for time-resolved measurements because it has a high flux multilayer monochromator capable of yielding over 10^{13} photons/sec. The scattered x rays were detected using a 2.5-cm-long linear diode array position sensitive detector with 1024 pixels [17] made by Princeton Instrument Inc. The position sensitive detector made it possible to obtain a high signal-to-noise ratio in the scattered intensity with a signal averaging times of 1 sec. A personal computer was used to control the position sensitive detector and store the intensity data at each pixel. The photon energy used was 6.8 keV, which corresponds to a wave-length of $\lambda = 1.8$ Å. The

detector was positioned approximately 95 cm away from the sample to obtain a maximum scattering angle of 1.5°, thus covering a wave number range of $0.004\ \text{Å}^{-1} < q < 0.075\ \text{Å}^{-1}$. The absolute incident beam intensity was monitored with a helium-filled chamber, and also independently determined by measuring the attenuated direct beam on the diode array detector. To measure the time evolution of the structure factor over the q range of interest following a temperature jump, the intensity was averaged for 1-sec, intervals, and these 1-sec scans were repeated over the duration of the phase separation process. The empty kapton cell scattering was carefully subtracted from the total scattering and the scattering patterns were normalized to an absolute scale per monomer using the ion chamber current to correct for any change of the incident beam intensity or sample absorption.

IV. RESULTS AND DISCUSSION

A. Equilibrium structure factor

According to the mean-field theory of a polymer in the one phase region, the structure factor of concentration fluctuations at low wave numbers is given by the Ornstein-Zernicke Lorentzian function

$$S_L(q) = \frac{S_L(0)}{1+\xi^2 q^2} \quad \text{for} \quad q\xi \ll 1. \tag{4}$$

Here $S_L(0)$ is the extrapolated structure factor at zero angle, and ξ is the correlation length of the concentration fluctuations. Systematic deviations from the Ornstein-Zernicke function have been reported at low $q's$ in equilibrium studies of polymer gels [6,18]. Although many attempts have been made to account for this effect, no conclusive explanation has been reached. Geissler *et al.* [18] proposed that the equilibrium structure factor of a gel can be described by a Lorentzian function plus a Gaussian function,

$$S(q) = S_G(0) e^{-\Xi^2 q^2} + \frac{S_L(0)}{1+\xi^2 q^2}. \tag{5}$$

The Gaussian part is associated with the solidlike contribution from the gel network, with Ξ denoting the average size of the solidlike nonuniformity. The absolute equilibrium structure factors ate temperatures 32.5 and 21.7 °C are presented in Fig. 1(a). Figure 1(b) displays the corresponding Zimm plots. The deviation from the straight line behavior characteristic of the Zimm plots is due to the excess scattering in the low q range. Figure 2 is a typical fit to the measured structure factors using Eq. (5).

As seen in Fig. 2, this is a good description of the equilibrium structure factor of the gel. The parameter $\Xi \sim 200$ Å is independent of the temperature. Since this parameter is related to the length scale of the pre-existing heterogeneities in the gel, the radius of gyration of the inhomogeneities, $R_{gi} = \sqrt{3}\Xi$, is approximately 340 Å. This calculation is based on the Guinier approximation, according to which the Gaussian part of the structure factor $\sim \exp(-q^2 R_{gi}^2/3)$. On the other hand, the correlation length of the concentration fluctuations ξ increases as T approaches T_s. Table I summarizes the parameters which fit the equilibrium

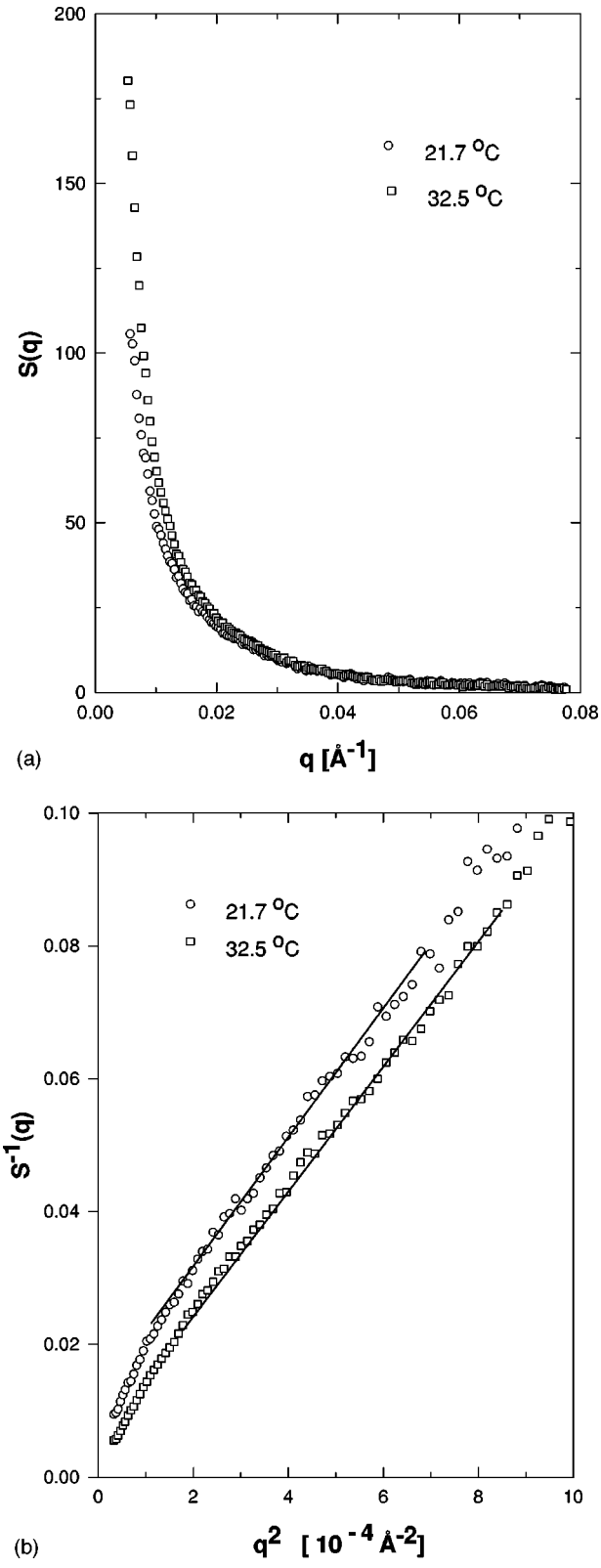

FIG. 1. (a) Equilibrium structure factors $S(q)$ vs q at two different temperatures. (b) The corresponding Zimm plots $S^{-1}(q)$ vs q^2.

structure factor at two temperatures. The values are larger than those obtained by Shibayama *et al.* [6] using SANS. The discrepancies are most likely due to the different q ranges of the SANS and SAXS experiments and to the fact that the samples they measured were swollen in D_2O to

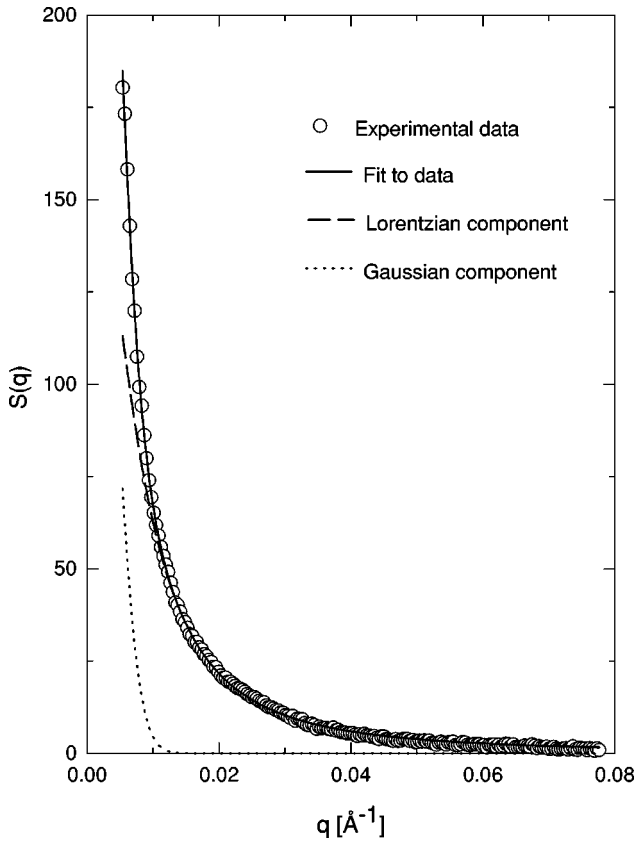

FIG. 2. A fit to the equilibrium structure factor $S(q)$ at 32.5 °C using Eq. (5).

slightly different final concentrations (5.8% and 8.3% as compared with our sample, which was used as prepared in H_2O at 7.8%). Another relevant length in a gel is the length of the primary chain between two crosslinks. Assuming that there are two primary chains per BIS monomer we determine the molecular weight M_w of the primary chain for the NIPA gel used in this study to be approximately 1850 Daltons. Kubota *et al.* [19] showed that the radius of gyration R_G (in Å) for NIPA is related to the molecular weight by $R_G = 0.22 M_w^{0.54}$. This gives $R_G = 12.7$ Å, which is much smaller than the correlation length ξ in the temperature range of interest ($\xi \sim 8R_G$ at 21.7 °C, and $\xi \sim 10R_G$ at 32.5 °C), and 16 times smaller than the size of the heterogeneities in the gel.

B. Spinodal decomposition kinetics

We performed a temperature jump from room temperature $T_i = 21.7$ °C to $T_f = 42.5$ °C. The temperature stabilized to less than ± 0.2 °C within 75 sec. In all subsequent discussion and figures, this equilibration time has been subtracted so that $t = 0$ corresponds to the time when the sample reaches the final temperature. From the dependence of the peak position on the quench temperature in time-resolved SALS experiments of NIPA gels [8], we estimate the peak position to be in the vicinity of $q_m = 0.3\ \mu\text{m}^{-1}$ for a quench to 42 °C, corresponding to micrometer size phase-separated domains. Since SAXS and SANS measurements probe wave numbers much higher than those covered in SALS (10^{-4} Å$^{-1} < q < 10^{-5}$ Å^{-1}), only the high-q tail of the structure factor's peak following a quench into the spinodal is observed in the SAXS experiment, as shown in Fig. 3(a). Figure 3(a) shows a clear growth of the intensity at these much higher wave numbers, corresponding to distance scales ranging from R_G of the primary chain in the gel to about twice the correlation

TABLE I. Equilibrium structural parameters of 7.8% NIPA gel.

T (°C)	$I_L(0)$	ξ(Å)	$I_G(0)$	Ξ(Å)
21.7	93.0	97.6	114.7	184.4
32.5	167.6	130.0	221.0	197.8

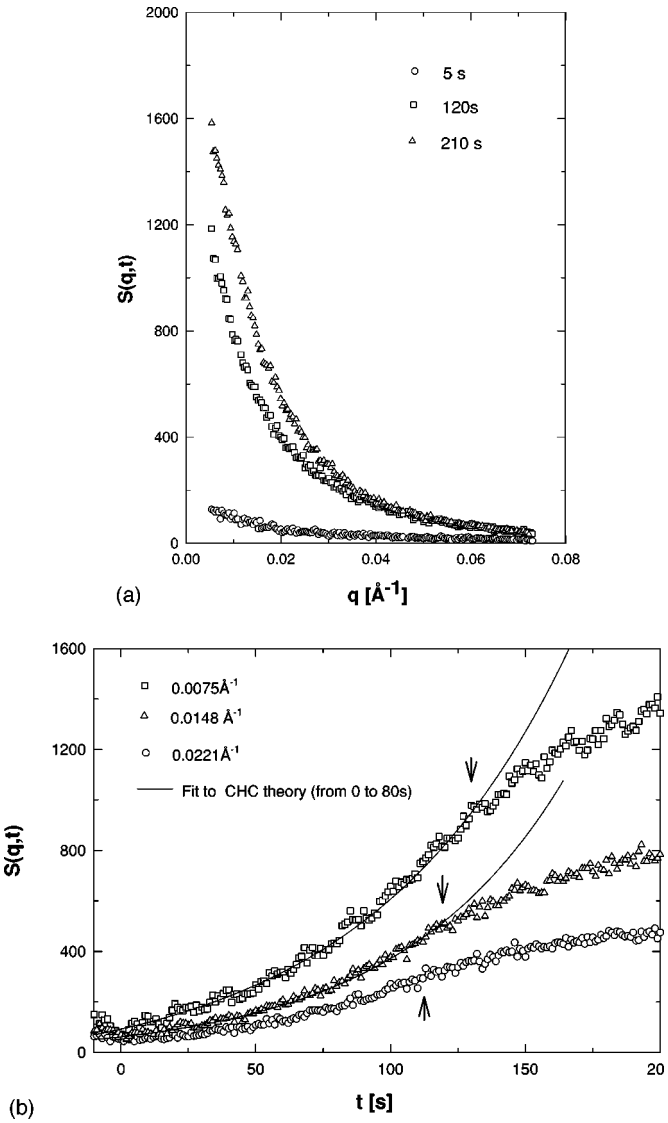

FIG. 3. (a) The structure factor $S(q,t)$ vs q at different times t as indicated, following a quench from 21.7 to 42.5 °C. The values of time indicated on the different scans are obtained after subtracting the time for the sample to reach the final temperature. (b) $S(q,t)$ vs t at different wave numbers, as indicated for the same quench as in 3(a). The solid lines are fit to Eq. (2). The data was fit over the time interval where the linear theory is valid, which was estimated by the linear region of $\partial S(q,t)/\partial t$ vs $S(q,t)$. This fitting time interval for the wave numbers indicated in the figure is from 0 to 80 s. The arrows indicate the breakdown of the CHC fit due to the onset of non-linearities.

length in the gel. Thus the growth in the SAXS intensity is a measure of internal scattering from concentration fluctuations within the domains.

Figure 3(b) shows the time evolution of the structure factor at three different wave numbers following the quench to 42 °C. Since the zero of time is taken as the time at which the sample's temperature has equilibrated, these data represent the isothermal time evolution of the structure factor. After an initial exponential growth seen at all the wave numbers, the structure factor appears to saturate. The saturation occurs earlier at the high wavenumbers than at low wavenumbers. In fact very little growth is seen at the highest wave numbers, which correspond to length scales comparable to the primary chain in the gel. In the following we separately discuss the time evolution at the early stages and the behavior in the vicinity of the final saturation.

C. Linear CHC analysis of early stage kinetics

The exponential growth seen at early times can be analyzed within the framework of the linear CHC theory. We fit the time evolution of the structure factor at fixed wave number directly to the exponential form of Eq. (2) in the early stage, as shown in Fig. 3(b). Both $R(q)$ and $S_\infty(q)$ are directly obtained as fitting parameters, and the Onsager coefficient $\Lambda(q)$ can be calculated by Eq. (3). In fitting data one has to be careful about the limited applicability of the CHC approach, and this requires a determination of the linear region before the fit is carried out. We determined the linear region by evaluating the derivative $\partial S(q,t)/\partial t$ at fixed wave number q and plotting $\partial S(q,t)/\partial t$ versus $S(q,t)$ with time t as an implicit variable. As seen from Eq. (1), this plot can directly be used to estimate the growth rate $R(q)$ and the Onsager coefficient $\Lambda(q)$ from the slope and intercept, respectively. However, since derivatives amplify any noise in the original data, we preferred to fit the original $S(q,t)$ data versus t over the linear region determined from the derivative analysis. As a further test of the reliability of our fitting procedure, we also analyzed our data using the ''1/3 power plot'' proposed by Sato and Han [20]. This approach works only when $R(q)t<1$. All three methods give similar values for the parameters $R(q)$ and $S_\infty(q)$ for those q-values where all methods could be reliably applied. In the remainder of this discussion, we use the results of the direct fit to the exponential form in Eq. (2).

A further issue in the data analysis concerns how to handle the pre-existing inhomogeneities modeled by the Gaussian term in the equilibrium structure factor [Eq. (5)]. The key issue here is whether concentration fluctuations due to pre-existing heterogeneities are amplified during the microphase separation process. The answer is unclear. However, the Langevin equation on which the Cahn-Hilliard model is based, and from which most of the relevant kinetic theory is derived, makes no distinction between thermal concentration fluctuations present at the time when the quench is initiated and other kinds of concentration fluctuations. However, in order to test how sensitive our results are to this question, we have also performed a CHC analysis with the preexisting heterogeneities subtracted out. This subtraction affects only $S_\infty(q)$ not $R(q)$. In fact $S_\infty(q)$ is simply decreased by the magnitude of the initial scattering due to the heterogeneity. Since this is very small, except at the lowest two or three q-values, the results are unchanged except at these lowest wave numbers.

As seen in Fig. 3(b), the fit to the CHC equation breaks down after some time. The time at which it breaks down is related to the onset of nonlinearities due to coupling of fluctuations of different wave numbers. The arrows in Fig. 3(b) indicate that the onset of nonlinearities occurs earlier at higher wave numbers, in agreement with recent theoretical predictions of Gross *et al.* [21].

D. q dependence of growth rate, virtual structure factor, and mobility

The growth rates $R(q)$ obtained from the exponential fit are plotted as function of q^2 for different quench temperatures in Fig. 4(a). Throughout the wave number range we studied, an approximate linear behavior in q^2 is observed, i.e., $R(q)\sim A-Bq^2$, where A and B are constants. A linear dependence of $R(q)$ on q^2 is in agreement with Binder's prediction [16] using mean-field arguments for spinodal decomposition in polymer blends. Since the modified Flory-Huggins free energy for the polymer gel is similar to the free energy in the polymer blend and the internal polymer dynamics in a gel are not likely to be different than in either a semidilute solution or an entangled melt, it is not surprising to observe similar behaviors in gels and blends.

The positive sign of $R(q)$ in this q range indicates that the concentration fluctuations probed here grow following a quench into the unstable region. As mentioned earlier, according to the linear CHC theory the growth rate $R(q)$ changes from positive to negative for $q>q_c$, with q_c representing the crossover wave number beyond which concentration fluctuations relax instead of exponentially growing. From the graph of $R(q)$ versus q^2, we obtain the crossover wave number as $q_c\cong 0.1$ Å^{-1}. Theories of spinodal decomposition suggest that $q_c\sim 1/\xi_-$, where the correlation length ξ_- at a given temperature difference from the spinodal $\Delta T = T_f - T_s$ in the two phase region can be related to the correlation length ξ_+ measured in the one phase region at the same temperature difference from the spinodal by $\xi_- = 0.524\xi_+$ (Ising model). From the work of Shibayama *et al.* [6] and our measurement of the equilibrium structure factor at 21 °C, we estimate that ξ_+ lies in the range 50–100 Å at 28 °C, which gives $\xi_-\approx 25$–50 Å$\gg 1/q_c$ at 42 °C. This discrepancy between the crossover wave number and the CHC prediction of $1/\xi$ has also been observed in time-resolved SANS studies of spinodal decomposition kinetics in polymer blends [10,11]. The crossover wave number q_c in the linear CHC theory is related to the peak position of scattering maximum $q_m$via $q_c=\sqrt{2}q_m$. At the value of $q_m = 0.07$ Å^{-1} predicted by this relationship, we do not observe any peak in the SAXS data. As mentioned earlier, the peak in the scattering lies in the SALS region, at a much lower wave number than probed by the SAXS experiments. Our observation that $q_m\ll q_c$ is consistent with the prediction of Binder [7], where he found that $q_m=q_c/\sqrt{2}$ holds only for shallow quenches whereas for deep quenches $q_m\ll q_c$. Interestingly, we find that $q_m R_g\sim 1$; whether this is a coincidence or a reflection of the role of chains between cross-links in the process of the phase separation can be determined by exam-

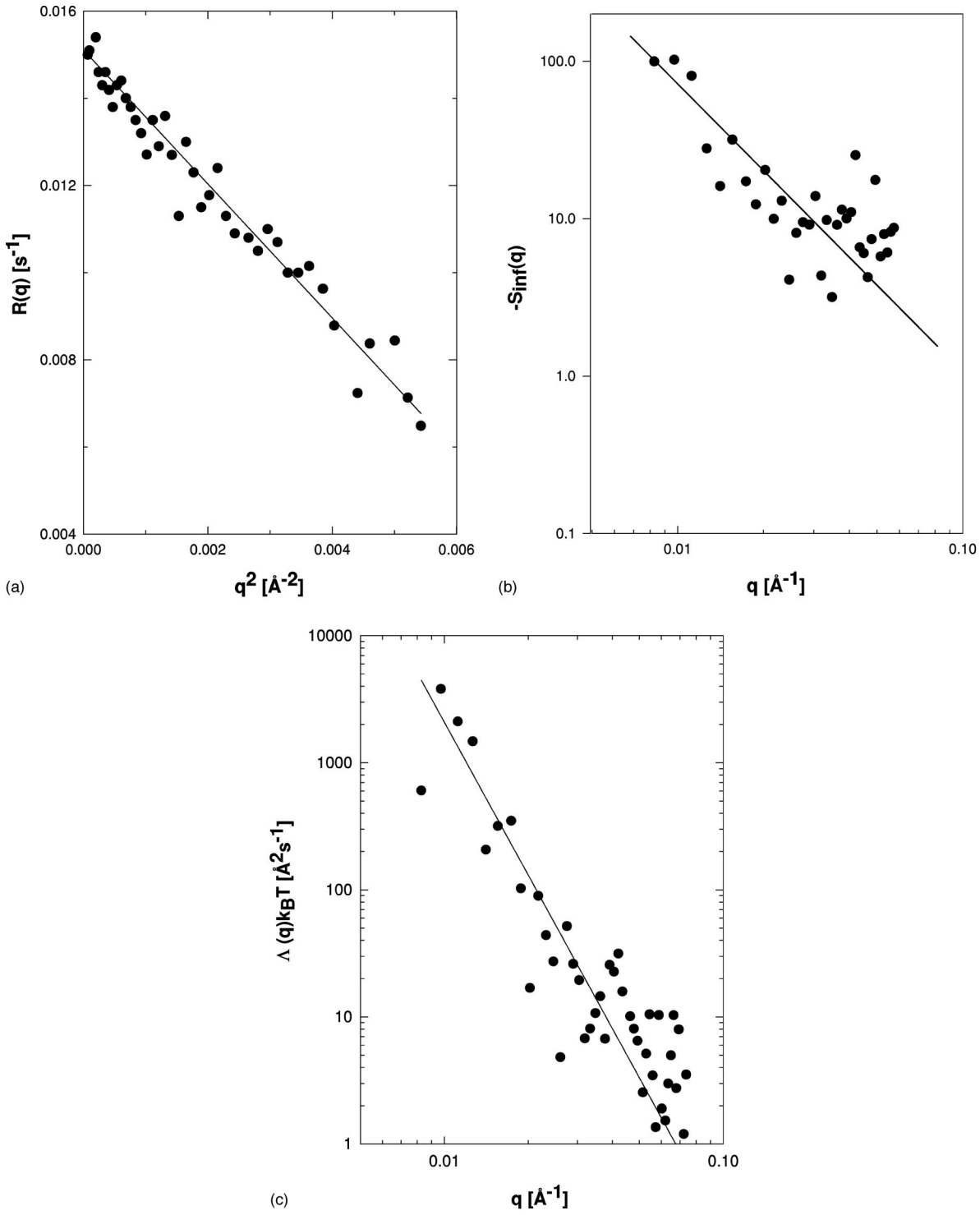

FIG. 4. (a) The growth rates $R(q)$ vs q^2 calculated from the CHC fit. The solid line is the best linear fit to the data. (b) A log-log plot showing the q dependence of the magnitude of the virtual structure factor $-S_\infty(q)$ evaluated from the CHC fit. The line with the slope of -2 is drawn as a guide to the eye. (c) The Onsager coefficient $\Lambda(q)k_BT$ vs q calculated from Eq. (3). The best fit of the data gives $\Lambda(q)\sim q^{-4}$, as shown by the solid line.

ining samples with different cross-link concentrations, which is beyond the scope of the present paper.

The q dependence of the virtual structure factor was obtained from the fit of $S(q,t)$ at fixed values of q. The Onsager coefficient was then calculated from Eq. (3). As expected for a quench into the spinodal region, the virtual structure factor is negative. We find that the magnitude of the virtual structure factor scales as $-S_\infty(q)\sim q^{-2}$, whereas the Onsager coefficient scales as $\Lambda(q)\sim q^{-4}$, as shown in Figs. 4(b) and 4(c), respectively. It is important to point out that using our empirical observations for $R(q)\sim A-Bq^2$ with $A>Bq^2$ and $-S_\infty(q)\sim q^{-2}$ in Eq. (3) we obtain $\Lambda(q)\sim Aq^{-4}-Bq^{-2}$. The q^{-4} behavior seen in Fig. 4(c) represents the leading factor at small $q's$; the correction term

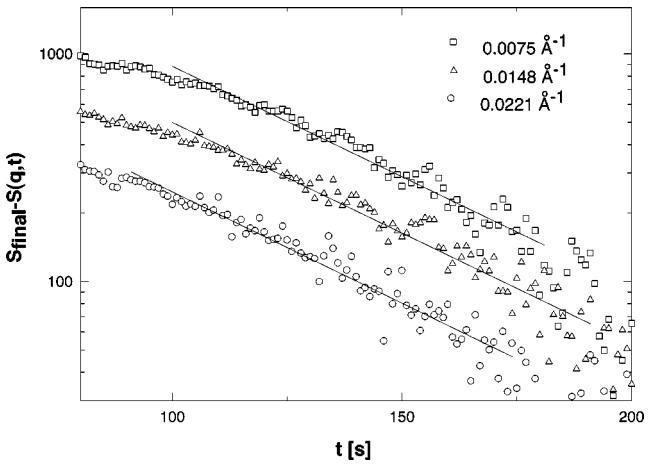

FIG. 5. The same experimental data as in Fig. 3(b) are plotted as $S_{\text{final}}(q,t)-S(q,t)$ on a logarithmic scale vs t to show the effects of saturation at late time. The straight lines indicate a regime where the data can be described as approaching the final saturation limit via an exponential relaxation process.

Bq^{-2} is relatively small except at large wave numbers, where the uncertainity in the data analysis is large. We also note that, over the measured wave number range, $S_{\infty}(q)$ changes by almost a factor of 25, whereas $R(q)$ changes only by a factor of 2. The strong q dependence of the Onsager coefficient $\Lambda(q)\sim q^{-4}$ was also observed in SAXS studies of polystyrene-dioctylphthalate solutions undergoing spinodal decomposition. However, in polymer blends, $\Lambda(q)\sim q^{-2}$ has been observed [10,11], which is consistent with theoretical predictions of polymer chain dynamics [7].

There is no theoretical explanation for such a strong q dependence of the nonlocal mobility. Perhaps the spinodal decomposition is enhanced by pre-existing inhomogeneities in the gel, which give rise to the stronger q dependence. This might also explain why the peak in the SALS data is at much smaller wave numbers than $1/\xi$ as predicted theoretically.

E. Saturation of structure factor at late times

At late stages there is a significant difference in the time evolution of $S(q,t)$ for the gel as compared to either a semidilute solution [9] or a blend [11]. In the latter cases the scattered intensity at fixed q's decreases after some time as the peak in $S(q,t)$ shifts closer to zero and the peak narrows. This is a direct consequence of the coarsening of domains at late times. In contrast to these observations we find that at all the $q's$ examined here the structure factor approaches a saturation limit S_{final} at late times. We know of no theoretical model which fits the time evolution of $S(q,t)$ over the entire time interval of this experiment. We have examined several empirical forms to describe the later stages of the time evolution leading to the saturation. We found that the approach to the saturation limit can be described reasonably well as an exponential relaxation. We estimated S_{final} by averaging the last 10–15 data points. This procedure works well for the higher q values. At the lower q's, there is some disagreement at the longest times, since the structure factor is still evolving slowly. As shown in Fig. 5, the linearity in the semi-log plot of $[S_{\text{final}}(q)-S(q,t)]$ versus t at late times is clearly consistent with an exponential relaxation to the final structure factor. The negative slope of this line indicates an exponential relaxation rate of $-K(q)$ with which the structure factor approaches the final saturation limit. This is in contrast to the positive exponential growth rate $R(q)$, which describes the growth of fluctuations at early times. As expected, the late-stage relaxation obviously breaks down at early times; the lines in Fig. 5 indicate the range of validity of this late-stage exponential relaxation regime. We find that the higher the wave number the faster is the saturation process, i.e., $K(q)$ increases with increasing wavenumber [See Fig. 6(a)]. A simple reason for this may be that at the highest wave numbers we observe scattering on length scales comparable to the average distance between the tetra-functional BIS cross-links. If the saturation represents pinning due to the presence of the gel mesh, then one might expect a faster pinning at these length scales and slower relaxation to a pinned morphology at distances larger than the gel mesh. Similar pinning effects have been reported in gels where gelation and spinodal decomposition occur simultaneously. Bansil *et al.* [22] observed exponential saturation in the physical gel of gelatin quenched to a temperature in the two phase region, where it undergoes phase separation and gelation simultaneously. Asnaghi *et al.* [23] investigated the polymerization of polyacrylamide gels with a high BIS cross-link content. In this system, as the polymerization proceeds, microphase separation of highly cross-linked clusters occurs. Turbidity measurements show an exponential saturation corresponding to the pinning of the microphase-separated domains.

The q-dependence of S_{final} is shown in Fig. 6(b). It can be described asymptotically as a Lorentzian with a negative intercept at zero q. This would indicate that the structure is pinned in a nonequilibrium morphology. We note that while the virtual structure factor S_{∞} is negative [see Fig. 4(b)], the final structure factor S_{final} is positive over the entire measured q range. The structure factor $S(q,t)$ can be decomposed into two contributions, $S(q,t)=S_{\text{SD}}(q,t)+S_{\text{internal}}(q,t)$, where S_{SD} arises from the interference between growing spinodally decomposed domains and S_{internal} arises from the local composition fluctuations [24]. At late times, in the region $q\gg q_c$ the contribution from the growing domains becomes negligible, and the scattering from the local composition fluctuations within the domains, $S_{\text{internal}}(q,t)$, is the dominant contribution. If the system is completely separated into two equilibrium states, then the internal scattering from the system is the sum of the scattering from the local fluctuations of two kinds of domains, both of which have reached equilibrium states and thus give a positive intercept for the Zimm plot. This was observed in the SANS experiment on the phase separation in a polymer blend [24]. In contrast to this behavior, we observe a negative intercept in Fig. 6(b), indicating that at least one kind of domain has not reached the equilibrium state in the gel, i.e., the system is pinned in a locally nonequilibrium morphology. From Fig. 6(b), we can also obtain a correlation length of 50 Å for this microphase-separated structure.

F. Comparison of SALS and SAXS results on kinetics

As mentioned previously, we have also analyzed SALS data on the kinetics of spinodal decomposition in NIPA gels [8] using the CHC theory. Since these two techniques cover

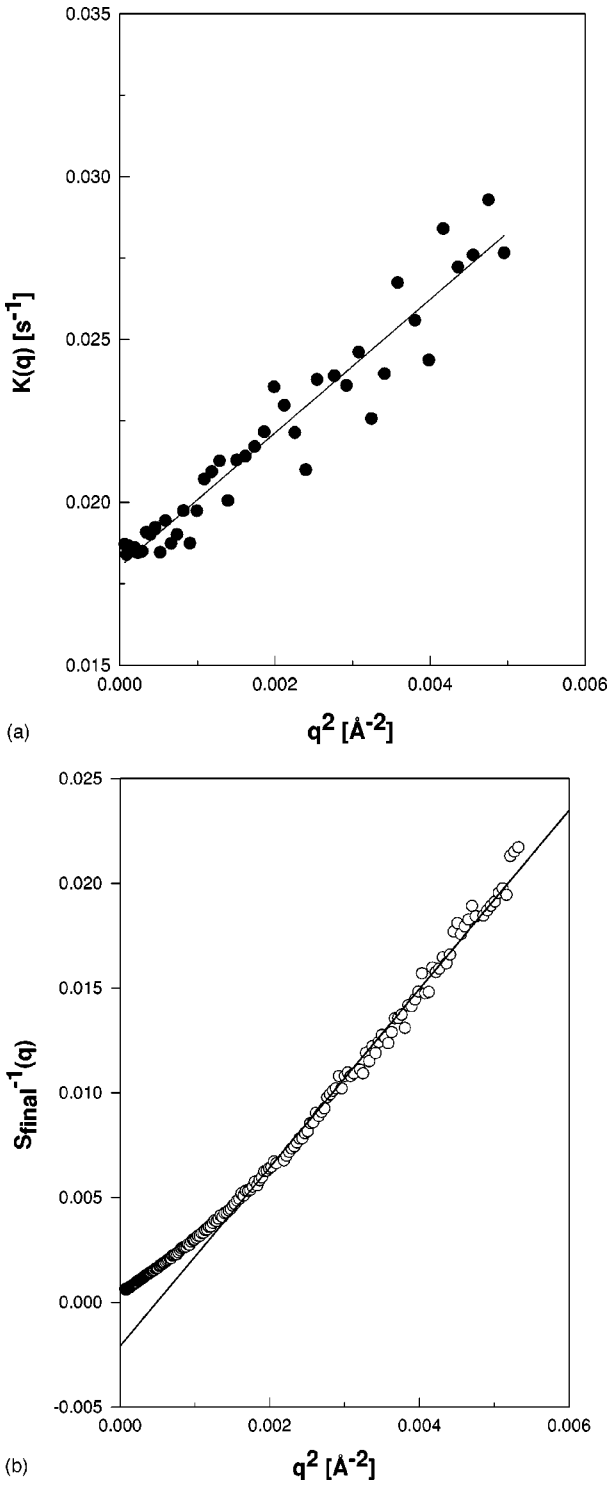

FIG. 6. (a) The wave number dependence of the relaxation rate $K(q)$. (b) The Zimm plot of the saturated intensity $S_{\text{final}}^{-1}(q)$ vs q^2, showing a clear negative intercept at $q=0$, implying that the structure of the gel is pinned in a microphase-separated, nonequilibrium state.

very different ranges in q,(10^{-4} Å$^{-1}<q<10^{-5}$ Å^{-1}) for SALS versus (10^{-2} Å$^{-1}<q<10^{-1}$ Å^{-1}) for SAXS they probe the time evolution of structure in spinodal decomposition on different length scales. Since the SALS experiments and SAXS experiments were performed on NIPA gels with the same total monomer concentration but with differing cross-link contents and different quench depths, only qualitative features can be compared. The most striking difference between these two measurements is that in the SALS data the structure factor shows a clear peak following a quench into the spinodal region, indicating that the characteristic domain sizes are in the range of micrometers. The SAXS data do not show a peak since they probe the time evolution of structure within these phase separating domains. The time evolution is much faster in the SAXS regime, in agreement with the usual observation of faster kinetics at smaller length scales. CHC analysis indicates that in both cases a positive growth rate was observed. The q dependence of the parameters is different in the two regimes. The growth rate is $R(q)\sim q^2$ in SAXS, and $R(q)/q^2\sim q^2$ in SALS. The mobility $\Lambda(q)$ is $\sim q^{-4}$ in the SAXS regime, whereas it is independent of q in the SALS regime. The q independence of the mobility and the q dependence of the growth rate for SALS are in accord with the mean-field predictions of Binder [16]. We know of no theoretical explanation of the observed q dependence of the SAXS results reported here. For both SALS and SAXS the linear CHC theory breaks down earlier at higher wave numbers; at the much higher wave numbers probed by SAXS this occurs around 100 s, whereas for SALS the linear theory holds for longer times, breaking down after approximately 500 s.

V. CONCLUSIONS

We have performed time-resolved SAXS measurements on a chemically cross-linked gel to examine the earliest steps in the volume collapse transition on length scales comparable to the average distance between cross-links and the correlation length of the gel. Our data show that the equilibrium structure factors seen in SAXS are in qualitative agreement with those reported from previous SANS studies of NIPA gels. We find that the early stages of the time evolution following a quench into the two phase spinodal region are in general agreement with the linear theory predictions. Whereas the quadratic q dependence of the growth rate is in agreement with the mean-field predictions of Binder [16], the growth rate remains positive for wavenumbers considerably higher than $1/\xi$. We also observe an unusually strong q dependence of the mobility, $\Lambda(q)\sim q^{-4}$, a result for which there is as yet no theoretical explanation. In contrast to the behavior of semidilute solutions and blends, at late times we observe a pinning of the structure factor. This relaxation to a final, microphase-separated morphology is faster and occurs earlier at the higher wave numbers, which probe length scales comparable to the distance between cross-links, suggesting that the microphase-separated morphology is pinned at these length scales first.

ACKNOWLEDGMENTS

This work was performed at the National Synchrotron Light Source, which is supported by the U.S. Department of Energy, Division of Material Science and Division of Chemical Sciences. R.B. acknowledges the support of the NSF Division of Materials Research.

[1] K. Dusek and D.J. Patterson, Polym. Sci. C **1**, 1209 (1968).
[2] T. Tanaka, Phys. Rev. Lett. **40**, 820 (1978).
[3] K. Sekimoto, Int. J. Mod. Phys. B **9**, 737 (1995), and references therein.
[4] S. Hirotsu, Y. Hirokawa, and T. Tanaka, J. Chem. Phys. **87**, 1392 (1987).
[5] S. Hirotsu, Phase Transit. **47**, 183 (1994).
[6] M. Shibayama, T. Tanaka, and C.C. Han, J. Chem. Phys. **97**, 6829 (1992).
[7] Y. Li, G. Wang, and Z. Hu, Macromolecules **28**, 4194 (1995).
[8] R. Bansil, G. Liao, and P. Falus, Physica A **231**, 346 (1996).
[9] Y. Xie, K.F. Ludwig, R. Bansil, P.D. Gallagher, C. Konak, and G. Morales, Macromolecules **29**, 6150 (1996).
[10] D. Schwahn, S. Janssen, and T. Springer, J. Chem. Phys. **97**, 8775 (1992).
[11] H. Jinnai, H. Hasegawa, T. Hashimoto, and C.C. Han, J. Chem. Phys. **99**, 8154 (1993).
[12] J.W. Cahn and J.E. Hilliard, J. Chem. Phys. **28**, 258 (1958).
[13] H.E. Cook, Acta Metall. **18**, 297 (1970).
[14] P.G. de Gennes, J. Chem. Phys. **72**, 4756 (1980).
[15] P. Pincus, J. Chem. Phys. **75**, 1996 (1981).
[16] K. Binder, J. Chem. Phys. **79**, 6387 (1983).
[17] G.B. Stephenson, K.F. Ludwig, J.L. Jordan-Sweet, S. Brauer, J. Mainville, Y.S. Yang, and M. Sutton, Rev. Sci. Instrum. **60**, 1537 (1989).
[18] E. Geissler, S. Mallam, A.M. Hecht, A.R. Rennie, and G. Horkay, Macromolecules **23**, 5270 (1990).
[19] K. Kubota, S. Fujishige, and I. Ando, Polym. J. (Tokyo) **22**, 15 (1990).
[20] T. Sato and C.C. Han, J. Chem. Phys. **88**, 2057 (1988).
[21] N. Gross, W. Klein, and K.F. Ludwig, Phys. Rev. Lett. **73**, 2639 (1994).
[22] R. Bansil, J. Lal, and B.L. Carvalho, Polymer **33**, 2961 (1992).
[23] D. Asnaghi, M. Giglio, A. Bossi, and P.G. Righetti, Macromolecules **30**, 6194 (1997).
[24] H. Jinnai, H. Hasegawa, T. Hashimoto, and C.C. Han, Macromolecules **24**, 282 (1991).